Estimation of Debris Hazard Areas due to a Space Vehicle Breakup at High Altitudes

Mahmut Reyhanoglu and Juan Alvarado
Physical Sciences Department
Embry-Riddle Aeronautical University
Daytona Beach, FL 32114, USA

Avishy Carmi
School of Mechanical and Aerospace Engineering
Nanyang Technological University
Singapore 639798

***Abstract*—With the recent developments in the Commercial Space Transportation industry, there has been a surge of interest in the analyses of the debris hazard areas due to a space vehicle breakup and the risk posed to the aircraft in the national airspace system as well as to the people and the property on the ground. The focus of this paper is to study the problem of estimation of the extent of the airspace containing falling debris due to a space vehicle breakup. A precise computation of propagation of debris to the ground is not practical for many reasons. There is insufficient knowledge of the initial state vector; ambient wind conditions; and key parameters, including the ballistic coefficient distributions. In addition, propagation of all debris pieces to the ground would require extensive computer time. In this paper, a computationally efficient covariance propagation method is employed for the estimation of debris dispersion.**

***Keywords*—Covariance propagation, estimation.**

I. INTRODUCTION

There has been considerable interest in studying the problem of the estimation of debris dispersion due to spacecraft disintegration. On-orbit spacecraft breakup models due to both collision and explosion, and the evolution of resulting space debris have been well studied in the literature ([2], [3], [9], [23]). A variety of methods have been employed to analyze the debris reentry trajectories ([7], [10], [11], [17], [22]) and to estimate the risk posed to people and the property on the ground ([4], [14], [15]).

Falling debris as a result of space vehicle breakup during ascent to orbit or descent from orbit poses a significant risk to aircraft ([16], [20]). Depending upon the altitude of the vehicle breakup, the physical properties of the pieces and the ambient conditions, some debris could impact the ground in a few minutes, while other debris capable of damaging or destroying an aircraft could continue to fall for the next couple hours ([5], [6]).

In our previous work [21], a covariance propagation method was introduced for the estimation of debris dispersion due to a space vehicle breakup during reentry. The concept of positional probability ellipsoids was utilized for the visualization of the simulation results. Through a case study, it was shown that while the results of the covariance propagation method are in close agreement with those of the Monte Carlo method, the covariance propagation method is much more computationally efficient than the Monte Carlo method. In [21], an average ballistic coefficient was assumed for all debris pieces. In this paper, we extend this work to the case in which the ballistic coefficient is a random variable that is independent of the other variables.

We apply the concept of positional probability ellipsoids to estimate the extent of the airspace containing falling debris due to a space vehicle breakup. Knowledge of debris hazard regions and their time duration would enable the air traffic managers and controllers to guide affected aircraft away from the hazard area before the debris from the breakup would reach the altitude at which aircraft are flying. The computation of hazard regions must be sufficiently conservative in accounting for uncertainties in both debris properties and ambient conditions to ensure that aircraft are adequately protected.

The 3D translational equations of motion for a particle with an average ballistic coefficient were integrated first to obtain a nominal trajectory using the state vector right before the breakup as the initial state. The equations of motion are then linearized around the nominal trajectory and the problem is formulated as a continuous Gauss-Markov process. Finally, a covariance propagation approach is applied to obtain the time evolution of the positional probability ellipsoids. Computer simulations are included to illustrate the results of the paper.

II. MATHEMATICAL FORMULATION

A. 3-D Translational Equations of Motion-Spherical Rotating Earth

Following the development in [21], let $x_1x_2x_3$ denote the topocentric horizon coordinate system at the breakup instant. The initial state (the state of the space vehicle right before the breakup) is given by the geometric altitude z_0, longitude θ_0, latitude ϕ_0, heading angle ψ_0 (measured from East counterclockwise), flight path angle γ_0, and (relative) speed v_0. The origin of the $x_1x_2x_3$ frame is at $(\theta_0,\, \phi_0)$ on the Earth's surface. The x_1x_2 plane is the local horizon, which is the plane tangent to the sphere at the origin. The x_3 axis is normal to this plane directed toward the zenith (i.e., the coordinate x_3 is the geometric altitude). The x_1 axis is directed eastward, and the x_2 axis points north. The $x_1x_2x_3$ frame is also referred to as ENZ (East-North-Zenith) frame.

Let $\boldsymbol{x} = [x_1,\, x_2,\, x_3]^T$ and $\boldsymbol{v} = [v_1,\, v_2,\, v_3]^T$ denote the position and (ground) velocity vectors, respectively, in the ENZ frame. Since $(\theta_0,\, \phi_0)$ locates the origin of the ENZ frame on the Earth's surface, the initial position is given by

$$(x_{1_0},\, x_{2_0},\, x_{3_0}) = (0,\, 0,\, z_0).$$

978-1-4673-5769-2/13/$31.00 ©2013 IEEE

Clearly, the initial velocity components in the ENZ frame can be computed as

$$\begin{aligned} v_{1_0} &= v_0 \cos\gamma_0 \cos\psi_0, \\ v_{2_0} &= v_0 \cos\gamma_0 \sin\psi_0, \\ v_{3_0} &= v_0 \sin\gamma_0. \end{aligned}$$

The ENZ frame rotates with an angular velocity of

$$\boldsymbol{\omega} = [\omega_1,\, \omega_2,\, \omega_3]^T = [0,\, \omega_e \cos\phi_0,\, \omega_e \sin\phi_0]^T,$$

where $\omega_e = 72.9217 \times 10^{-6}$ rad/s is the Earth's rotation rate.

Denote the air velocity by $\boldsymbol{v}_a = \boldsymbol{v} - \boldsymbol{w}$, where $\boldsymbol{w}$ is the wind velocity that depends on the position and possibly time. Then, the drag force is expressed as

$$\boldsymbol{D} = \frac{1}{2} C_D A \rho v_a \boldsymbol{v}_a,$$

where C_D is the drag coefficient, A is the reference area (usually the maximum cross-sectional area), ρ is the atmospheric density at the altitude x_3, and $v_a = \sqrt{\boldsymbol{v}_a^T \boldsymbol{v}_a}$ is the magnitude of the air velocity. Ignoring the lift force and including the gravity and drag forces only, the motion of a particle of mass M can be described by the following equations:

$$\dot{\boldsymbol{x}} = \boldsymbol{v}, \tag{1}$$

$$\dot{\boldsymbol{v}} = -\frac{\boldsymbol{D}}{M} - g\boldsymbol{e}_3 - 2\boldsymbol{\omega} \times \boldsymbol{v} - \boldsymbol{\omega} \times [\boldsymbol{\omega} \times (\boldsymbol{x} + r_e \boldsymbol{e}_3)] + \boldsymbol{\xi}, \tag{2}$$

where $r_e = 6378 \times 10^3$ m is the Earth's radius, $\mathbf{e}_3 = [0,\, 0,\, 1]^T$ is the third standard basis vector in $\mathbb{R}^3$, $\boldsymbol{\xi}$ is the random acceleration vector due to modeling uncertainties and disturbances, and

$$\beta = \frac{M}{C_D A}$$

denotes the ballistic coefficient, which is assumed to be constant for a given particle.

Let g_e denote the gravitational acceleration at zero altitude. Then according to the inverse square gravity model we have

$$g = g_e \left(\frac{r_e}{r_e + x_3} \right)^2.$$

A simple analytical atmosphere model is the exponential atmosphere model [19] given by

$$\rho = \rho_e e^{-x_3/H}, \tag{3}$$

where $\rho_e = 1.752$ kg/m^3 and $H = 6.7 \times 10^3$ m.

Let $\boldsymbol{s} = [\boldsymbol{x}^T,\, \boldsymbol{v}^T]^T$ and rewrite equations (1) and (2) in the form

$$\dot{\boldsymbol{s}} = \boldsymbol{f}(\boldsymbol{s}, t) + \boldsymbol{B}_s \boldsymbol{\xi}, \tag{4}$$

where

$$\boldsymbol{B}_s = \begin{bmatrix} \mathbf{0}_{3\times 3} \\ \mathbf{I}_{3\times 3} \end{bmatrix}.$$

In our previous work [21], we have assumed that the ballistic coefficients of all debris particles equal an average ballistic coefficient $\bar{\beta}$. In this paper, we extend our work to the case in which the ballistic coefficient is a random variable that is independent of the other variables. Therefore, in what follows we append the equation

$$\dot{\beta} = 0 \tag{5}$$

to (4) and consider the complete system defined by equations (4) and (5).

B. Linearized Equations of Motion

Let $\bar{s}(t)$ denote the nominal trajectory obtained by integrating the nonlinear equations of motion (4) by using the position and velocity of the vehicle right before the breakup as the initial state for a particle with average ballistic coefficient $\beta = \bar{\beta}$. Let $\boldsymbol{y} = [\boldsymbol{s}^T,\, \beta]^T$ and introduce the perturbation vector

$$\boldsymbol{z} = \boldsymbol{y} - \bar{\boldsymbol{y}} = \begin{bmatrix} \boldsymbol{s} - \bar{\boldsymbol{s}} \\ \beta - \bar{\beta} \end{bmatrix}. \tag{6}$$

Assuming that wind velocity depends on position only, i.e., $\boldsymbol{w} = \boldsymbol{w}(\boldsymbol{x})$, the linearized equations can be obtained as

$$\dot{\boldsymbol{z}} = \boldsymbol{A}(t)\boldsymbol{z} + \boldsymbol{B}\boldsymbol{\xi}, \tag{7}$$

where

$$\boldsymbol{A}(t) = \begin{bmatrix} \boldsymbol{A}_1(t) & \boldsymbol{A}_2(t) \\ \mathbf{0}_{1\times 6} & 0 \end{bmatrix},$$

with

$$\boldsymbol{A}_1(t) = \frac{\partial \boldsymbol{f}}{\partial \boldsymbol{s}}(\bar{\boldsymbol{y}}(t)) = \begin{bmatrix} \mathbf{0}_{3x3} & \mathbf{I}_{3x3} \\ \mathbf{F}(\bar{\boldsymbol{y}}(t)) + \mathbf{F}_e & \mathbf{G}(\bar{\boldsymbol{y}}(t)) + \mathbf{G}_e \end{bmatrix},$$

$$\boldsymbol{A}_2(t) = \frac{\partial \boldsymbol{f}}{\partial \beta}(\bar{\boldsymbol{y}}(t)) = \frac{\rho}{2\bar{\beta}^2} \bar{v}_a \bar{\boldsymbol{v}}_a,$$

and

$$\boldsymbol{B} = \begin{bmatrix} \boldsymbol{B}_s \\ \mathbf{0}_{1\times 3} \end{bmatrix}.$$

Here $\mathbf{F}(\boldsymbol{y})$ and $\mathbf{G}(\boldsymbol{y})$ are 3×3 matrix functions given by

$$F_{ij}(\boldsymbol{y}) = \frac{1}{2\beta} \left[\rho \left(\frac{v_{a_i}}{v_a} \boldsymbol{v}_a^T \frac{\partial \boldsymbol{w}}{\partial x_j} + v_a \frac{\partial w_i}{\partial x_j} \right) - \frac{\partial \rho}{\partial x_j} v_a v_{a_i} \right],$$

$$G_{ij}(\boldsymbol{y}) = -\frac{\rho}{2\beta} \left[\frac{v_{a_i} v_{a_j} + v_a^2 \delta_{ij}}{v_a} \right],\ i,\, j = 1,\, 2,\, 3,$$

and

$$\mathbf{F}_e = \begin{bmatrix} \omega_e^2 & 0 & 0 \\ 0 & \omega_e^2 \sin^2\phi_0 & -\omega_e^2 \sin\phi_0 \cos\phi_0 \\ 0 & -\omega_e^2 \sin\phi_0 \cos\phi_0 & \omega_e^2 \cos^2\phi_0 \end{bmatrix},$$

$$\mathbf{G}_e = \begin{bmatrix} 0 & 2\omega_e \sin\phi_0 & -2\omega_e \cos\phi_0 \\ -2\omega_e \sin\phi_0 & 0 & 0 \\ 2\omega_e \cos\phi_0 & 0 & 0 \end{bmatrix}.$$

Here δ_{ij} denotes the Kronecker delta.

III. Covariance Propagation Method

Consider the linearized equation (7) and let $\boldsymbol{\xi}(t)$ denote a vector of Gaussian white noise inputs. Then equation (7) with Gaussian initial conditions represents a continuous Gauss-Markov process [12] with the following specifications:

$$\boldsymbol{z}(0) = \mathcal{N}[\bar{\boldsymbol{z}}_0,\, \boldsymbol{Z}_0],$$

$$\mathrm{E}[\boldsymbol{\xi}(t)] = \bar{\boldsymbol{\xi}}(t),$$

$$\mathrm{E}[\boldsymbol{\xi}(t) - \bar{\boldsymbol{\xi}}(t)][\boldsymbol{\xi}(\tau) - \bar{\boldsymbol{\xi}}(\tau)]^T = \boldsymbol{\Xi}(t)\delta(t-\tau).$$

Here $\boldsymbol{\Xi}(t)$ denotes the white noise density. Throughout the paper, it is assumed that the random initial conditions are uncorrelated with the random inputs. The state vector $\boldsymbol{z}(t)$ is then Gaussian with mean vector $\bar{\boldsymbol{z}}(t)$ and covariance matrix $\boldsymbol{Z}(t)$, where

$$\dot{\bar{\boldsymbol{z}}} = \boldsymbol{A}(t)\bar{\boldsymbol{z}} + \boldsymbol{B}\bar{\boldsymbol{\xi}}(t), \tag{8}$$

$$\dot{\boldsymbol{Z}} = \boldsymbol{A}(t)\boldsymbol{Z} + \boldsymbol{Z}\boldsymbol{A}^T(t) + \boldsymbol{B}\boldsymbol{\Xi}(t)\boldsymbol{B}^T, \tag{9}$$

with initial conditions $\bar{\boldsymbol{z}}(0) = \boldsymbol{z}_0$ and $\boldsymbol{Z}(0) = \boldsymbol{Z}_0$. Note that the mean vector and covariance matrix are computed as

$$\bar{\boldsymbol{z}}(t) = \mathrm{E}[\boldsymbol{z}(t)],$$

$$\boldsymbol{Z}(t) = \mathrm{E}[\boldsymbol{z}(t) - \bar{\boldsymbol{z}}(t)][\boldsymbol{z}(t) - \bar{\boldsymbol{z}}(t)]^T.$$

The objective is to obtain positional probability ellipsoids that provide an estimate of debris dispersion through altitude layers. Since

$$\boldsymbol{x}(t) = \boldsymbol{C}\boldsymbol{z}(t),$$

where

$$\boldsymbol{C} = [\ \mathbf{I}_{3x3} \quad \mathbf{0}_{3x4}\ ],$$

the positional mean vector and the covariance matrix can be computed as

$$\bar{\boldsymbol{x}}(t) = \boldsymbol{C}\bar{\boldsymbol{z}}(t),\ \boldsymbol{X}(t) = \boldsymbol{C}\boldsymbol{Z}(t)\boldsymbol{C}^T.$$

In order to estimate the debris hazard areas, a statistical analysis is performed on the falling debris data to create a 3D probability volume that evolves with time by following the procedure summarized in Appendix A.

IV. Simulations

This section illustrates the main ideas through a covariance propagation analysis based on the linearized equations. The simulations were carried out using the widely accepted empirical density model MSISE-00 (Mass Spectrometer Incoherent Scatter Radar Extended 2000 [18]) and the wind model HWM-07 (Horizontal Wind Model 2007 [1]). As shown in [21], a significant reduction in computation time can be achieved using the covariance proagation method as opposed to the Monte Carlo method while retaining a high level of accuracy. These high fidelity density and wind models are described in Appendix B. Moreover, for simplicity it is assumed that the random acceleration vector $\boldsymbol{\xi}$ is negligible.

The simulations were carried out with the initial state (the state of the space vehicle right before the breakup) given by $z_0 = 78$ km, $\psi_0 = 0$, $\gamma_0 = -1^o$, $v_0 = 7.1$ km/s. The initial longitude and latitude were taken as $\theta_0 = 157^o$ W and $\phi_0 = 20^o$ N, respectively. The nonlinear equations (4) were first numerically integrated with these initial conditions and the average ballistic coefficient $\bar{\beta} = 5$ kg/m^2 to obtain a nominal trajectory. Then the equations of motion were linearized around the nominal trajectory and the problem was formulated as a continuous Gauss-Markov process. Finally, the covariance propagation approach described in Section 3 was employed to obtain the time evolution of the covariance matrix.

It is assumed that all the debris pieces have the same initial positions and vary only the initial velocity components and ballistic coefficients. An incremental speed of $\Delta v = 100$ m/s was added to $\boldsymbol{v}_0$ in every direction uniformly by creating a spherical grid of $32\times32 = 1024$ points (32 points for longitude and 32 points for latitude), i.e. $n = 1024$ different initial velocities were created using

$$\boldsymbol{v}_{ij_0} = \boldsymbol{v}_0 + \Delta v \begin{bmatrix} \cos\phi_i \cos\theta_j \\ \cos\phi_i \sin\theta_j \\ \sin\phi_i \end{bmatrix},$$

where $\phi_i \in [-pi/2,\, \pi/2),\ \theta_j \in [0,\, 2\pi),\ i, j = 1, \cdots, 32$. The variances for initial velocity components were computed as

$$\left(\sigma_1^2,\, \sigma_2^2,\, \sigma_3^2\right) = (0.0025,\, 0.0025,\, 0.0053)\ \frac{\mathrm{km}^2}{\mathrm{s}^2}.$$

The initial mean velocity vector was determined as

$$\bar{\boldsymbol{v}}_0 = \begin{bmatrix} v_{1_0} \\ v_{2_0} \\ v_{3_0} \end{bmatrix} = v_0 \begin{bmatrix} \cos\gamma_0 \cos\psi_0 \\ \cos\gamma_0 \sin\psi_0 \\ \sin\gamma_0 \end{bmatrix} = \begin{bmatrix} 7.099 \\ 0 \\ -0.1239 \end{bmatrix} \frac{\mathrm{km}}{\mathrm{s}},$$

Simulations were performed with different values for the ballistic coefficient variance σ_β^2.

The initial covariance matrix was chosen as

$$\boldsymbol{Z}_0 = \begin{bmatrix} \mathbf{0}_{3\times3} & \mathbf{0}_{3\times4} \\ \mathbf{0}_{4\times3} & \boldsymbol{Z}_{v\beta_0} \end{bmatrix},$$

where

$$\boldsymbol{Z}_{v\beta_0} = \mathrm{diag}\{\sigma_1^2,\, \sigma_2^2,\, \sigma_3^2,\, \sigma_\beta^2\}.$$

Here σ_β^2 denotes the ballistic coefficient variance.

Figs. 1-3 display the probability ellipsoids corresponding to a confidence interval of 99.99% for a sequence of time instants for $\sigma_\beta^2 = 1,\, 2,\, 3$ kg^2/m^4.

V. Conclusions

In this paper, a covariance propagation method has been proposed for the estimation of debris dispersion due to a space vehicle breakup at high altitudes. A spherical rotating Earth has been assumed and the inverse square gravity model has been used for the variation of the gravitational acceleration with altitude. The ballistic coefficient for the debris pieces has been modeled as an independent random variable. The concept of positional probability ellipsoids has been employed for the visualization of the simulation results corresponding to different ballistic coefficient variances.

Future research includes debris dispersion problems incorporating random acceleration vectors, lift forces, and the physical properties of the debris such as materials and temperatures into the model.

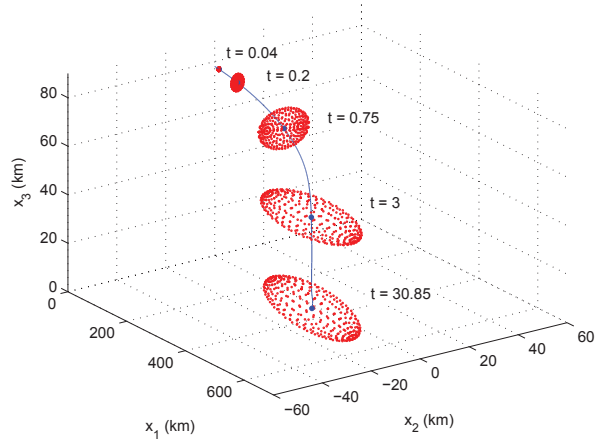

Figure 1. Probability ellipsoids for a sequence of time instants ($\sigma_\beta^2 = 1\ \mathrm{kg}^2/\mathrm{m}^4$).

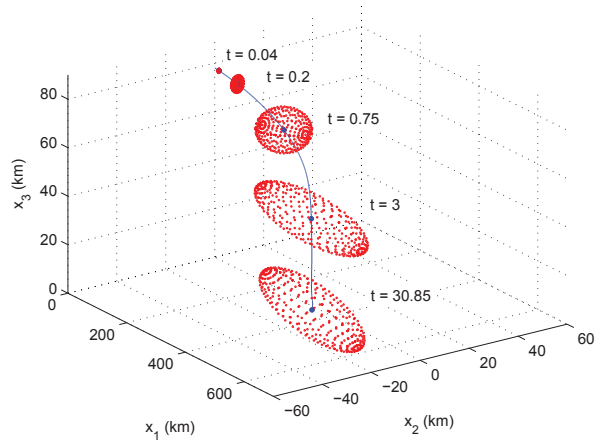

Figure 2. Probability ellipsoids for a sequence of time instants ($\sigma_\beta^2 = 2\ \mathrm{kg}^2/\mathrm{m}^4$).

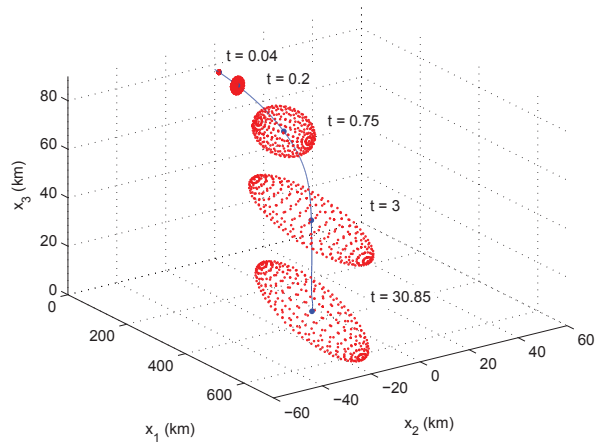

Figure 3. Probability ellipsoids for a sequence of time instants ($\sigma_\beta^2 = 3\ \mathrm{kg}^2/\mathrm{m}^4$).

Appendix A: Statistical Analysis

The positional multivariate Gaussian or multivariate normal probability density is given by [13]:

$$p(\boldsymbol{x}, t) = \frac{\exp\left[-\frac{1}{2}[\boldsymbol{x}(t) - \bar{\boldsymbol{x}}(t)]^T \boldsymbol{X}^{-1}(t)[\boldsymbol{x}(t) - \bar{\boldsymbol{x}}(t)]\right]}{(2\pi)^{3/2}|\boldsymbol{X}(t)|^{1/2}}.$$

The quadratic form

$$[\boldsymbol{x}(t) - \bar{\boldsymbol{x}}(t)]^T \boldsymbol{X}^{-1}(t)[\boldsymbol{x}(t) - \bar{\boldsymbol{x}}(t)] = \delta^2$$

defines the Mahalanobis distance δ between $\boldsymbol{x}$ and $\bar{\boldsymbol{x}}$. The equation δ^2 =const defines ellipsoids, which are the level sets of constant density. In what follows, we will drop the argument t for notational simplicity.

The eigenvectors $\boldsymbol{u}_i$ and eigenvalues λ_i of the positive definite covariance matrix $\boldsymbol{X}$ can be computed via solving the eigenvalue problem:

$$\boldsymbol{X}\boldsymbol{u}_i = \lambda_i \boldsymbol{u}_i.$$

Let $\boldsymbol{U}$ be the square matrix whose columns are the eigenvectors and let

$$\boldsymbol{\Lambda} = \mathrm{diag}\{\lambda_1, \lambda_2, \lambda_3\}.$$

Then the positional covariance matrix can be expressed as

$$\boldsymbol{X} = \boldsymbol{U}\boldsymbol{\Lambda}\boldsymbol{U}^T.$$

Now consider the transformation

$$\boldsymbol{x} = \bar{\boldsymbol{x}} + \boldsymbol{U}\boldsymbol{\Lambda}^{1/2}\boldsymbol{p}. \tag{10}$$

The mean vector and the covariance matrix of the random vector $\boldsymbol{p}$ can be computed as

$$\bar{\boldsymbol{p}} = 0,$$

$$\boldsymbol{P} = \mathrm{E}(\boldsymbol{p} - \bar{\boldsymbol{p}})(\boldsymbol{p} - \bar{\boldsymbol{p}})^T = \boldsymbol{I}.$$

Using the fact that $\boldsymbol{X}^{-1} = \boldsymbol{U}\boldsymbol{\Lambda}^{-1}\boldsymbol{U}^T$, the contours of constant probability density can be expressed as

$$p_1^2 + p_2^2 + p_3^2 = \delta^2.$$

The Mahalanobis distance δ that corresponds to a given confidence interval $c \in [0\ 1]$ can be computed using Matlab's inverse χ^2 function as $\delta^2 = \mathrm{chi2inv}(c, 3)$.

Note that the $\boldsymbol{p}$-sphere can be parameterized as

$$\boldsymbol{p} = \begin{bmatrix} p_1 \\ p_2 \\ p_3 \end{bmatrix} = \begin{bmatrix} \delta\cos\lambda\cos\alpha \\ \delta\cos\lambda\sin\alpha \\ \delta\sin\lambda \end{bmatrix},$$

where $\lambda \in [-\pi/2\ \ \pi/2]$ and $\alpha \in [0\ \ 2\pi]$. Now the probability ellipse for the $\boldsymbol{x}$ variables can be parameterized by using (10).

APPENDIX B: EMPIRICAL DENSITY AND WIND MODELS

Here we briefly summarize the widely accepted empirical density model MSISE-00 (Mass Spectrometer Incoherent Scatter Radar Extended 2000) and the wind model HWM-07 (Horizontal Wind Model 2007). Fig. 4 shows comparison of analytical and empirical density models. Fig. 5 shows eastern and northern wind profiles for different altitudes (see also [21]).

We simulated the nonlinear equations (1) and (2) for different ballistic coefficients using the empirical density and wind models. The same initial conditions as in Section 4 were used in the simulations. Fig. 6 shows the plot of flight time versus ballistic coefficient.

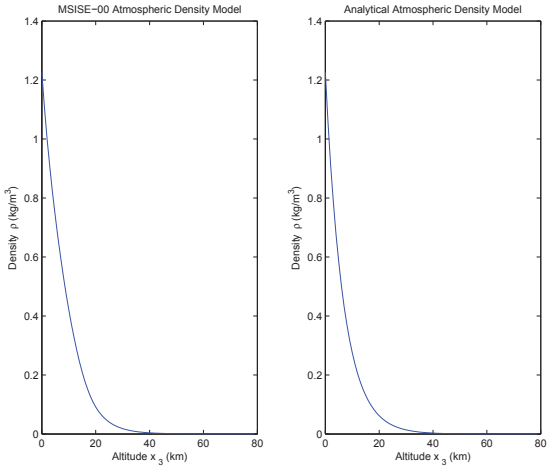

Figure 4. Density profiles for the MSISE-00 and the analytical atmospheric models.

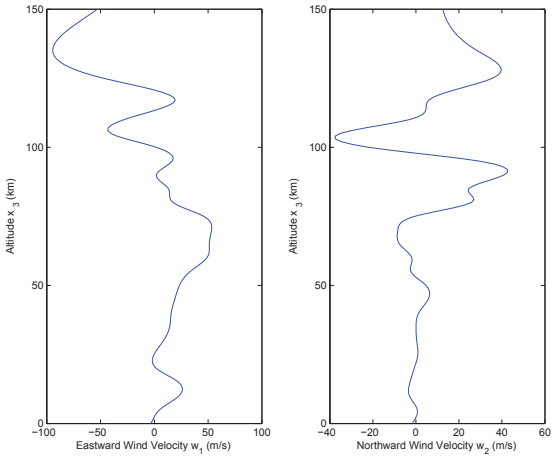

Figure 5. Eastward and northward wind profiles for different altitudes.

ACKNOWLEDGMENTS

This research was partially supported by FAA under OTA#DTFAWA-11-A-00002.

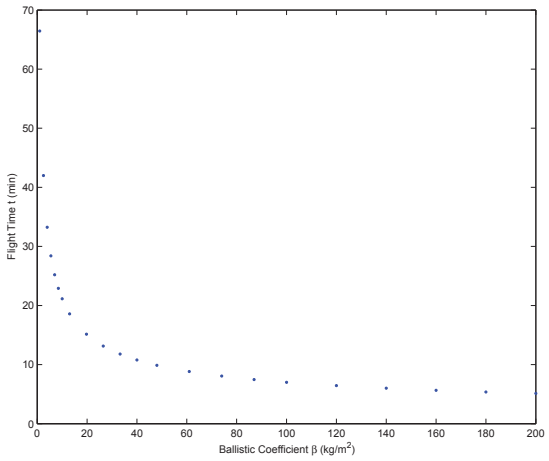

Figure 6. Flight times for different ballistic coefficients (empirical density and wind).

REFERENCES

[1] Alken, P., Maus. S., Emmert, J., and Drob, D. P., "Improved Horizontal Wind Model HWM07 Enables Estimation of Equatorial Ionospheric Electric Fields from Satellite Magnetic Measurements," *Geophysical Research Letters*, Vol. 35, L11105, doi:10.1029/2008GL033580, 2008.

[2] A. K. Anilkumara, M. R. Ananthasayanamb, P. V. Subba Raoa, "Aposterior Semi-stochastic Low Earth Debris On-orbit Breakup Simulation Model," *Acta Astronautica*, Vol. 57, pp. 733-746, 2005.

[3] M. R. Ananthasayanamb, A. K. Anilkumara, P. V. Subba Raoa, "New Approach for the Evolution and Expansion of Space Debris Scenario," *Journal of Spacecraft and Rockets*, Vol. 43, No. 6, pp. 1271-1282, 2006.

[4] L. Anselmo and C. Pardini, "Computational Methods for Reentry Trajectories and Risk Assessment," *Advances in Space Research*, Vol. 35, No. 7, pp. 1343-1352, 2005.

[5] J. B. Baeker, J. D. Collins, and J. M. Haber, "Launch Risk Analysis," *Journal of Spacecraft and Rockets*, Vol. 14, No. 12, pp. 733-738, 1977.

[6] J. D. Collins, R. Nyman, and I. Lottati,"Estimation of Space Shuttle Orbiter Reentry Debris Casualty Area," *Proceedings of the AIAA Atmospheric Flight Mechanics Conference and Exhibit*, August 2005, AIAA-2005-6321.

[7] R. Crowther, "Re-entry Aerodynamics Derived from Space Debris Trajectory Analysis," *Planetary and Space Science*, Vol. 40, No. 5, pp. 641-646, 1992.

[8] FAA Report, Concept of Operations for Global Space Vehicle Debris Threat Management, 2010.

[9] B. Fritsche, G. Koppenwallner, and T. Lips, "Modeling of Spacecraft Explosions During Re-entry," *Science and Technology Series*, Vol. 110, pp. 157-169, 2005.

[10] B. Fritsche, H. Klinkrad, A. Kashkovsky, and E. Grinberg, "Spacecraft Disintegration During Uncontrolled Atmospheric Reentry," *Acta Astronautica*, Vol. 47, No. 2, pp. 513-522, 2000.

[11] B. Fritsche, T. Lips, and G. Koppenwallner, "Analytical and Numerical Re-entry Analysis of Simple-Shaped Objects," *Acta Astronautica*, Vol. 60, No. 8-9, pp. 737-751, 2007.

[12] C. W. Gardiner, *Handbook of Stochastic Methods*, Springer-Verlag, Berlin, 2003.

[13] R. A. Johnson and D. W. Wicherin, *Applied Multivariate Statistical Analysis*, Prentice Hall, New Jersey, 2002.

[14] H. Klinkrad, "Assessment of the On-ground Risk During Re-entries," *Proceedings of the 3rd European Conference on Space Debris*, 2001, pp. 507-514.

[15] H. Klinkrad, B. Fritsche, and T. Lips, "A Standardized Method for Re-entry Risk Evaluation," *Science and Technology Series*, Vol. 110, pp. 141-155, 2005.

[16] E. W. F. Larson, S. L. Carbon, and D. P. Murray,"Automated Calculation of Aircraft Hazard Areas from Space Vehicle Accidents: Application to the Shuttle," *Proceedings of the AIAA Atmospheric Flight Mechanics Conference and Exhibit*, August 2008, AIAA-2008-6889.

[17] T. Lips and B. Fritsche, "A Comparison of Commonly Used Re-entry Analysis Tools," *Acta Astronautica*, Vol. 57, No. 2-8, pp. 312-323, 2005.

[18] Picone, J. M., Hedin, A. E., Drob, D. P., and Aikin, A. C., "NRLMSISE-00 Empirical Model of the Atmosphere: Statistical Comparisons and Scientific Issues," *Journal of Geophysical Research*, Vol. 107, No. A12, 1468, doi:10.1029/2002JA009430, 2002.

[19] F. J. Regan and S. M. Anandakrishnan, *Dynamics of Atmospheric Re-Entry*, AIAA Education Series, Washington, DC, 1993.

[20] M. Reyhanoglu, S. Drakunov, and J. Alvarado," Feasibility of Space Vehicle Debris Hazard Airspace Stratification," *Proceedings of the AIAA Space 2011*, September 2011, AIAA-2011-7182.

[21] M. Reyhanoglu and J. Alvarado,"Estimation of Debris Dispersion due to a Space Vehicle Breakup During Reentry," *Acta Astronautica*, Vol. 86, pp. 211-218, 2013.

[22] W. C. Rochelle, J. J. Marichalar, and N. L. Johnson, "Analysis of Reentry Survivability of UARS Spacecraft," *Advances in Space Research*, Vol. 34, No. 5, pp. 1049-1054, 2004.

[23] L. Wang and P. W. Stark, "Direct Simulation of Space Debris Evolution," *Journal of Spacecraft and Rockets*, Vol. 36, No. 1, pp. 114-123, 1999.